

Drone-based quantum key distribution

Xiao-Hui Tian^{1*}, Ran Yang^{1*}, Ji-Ning Zhang¹, Hua Yu², Yao Zhang¹, Pengfei Fan¹, Mengwen Chen¹, Changsheng Gu¹, Xin Ni¹, Mingzhe Hu¹², Xun Cao¹, Xiaopeng Hu¹, Gang Zhao¹², Yan-Qing Lu¹, Zhi-Jun Yin², Hua-Ying Liu¹⁺, Yan-Xiao Gong¹⁺, Zhenda Xie¹²⁺, and Shi-Ning Zhu¹

1. National Laboratory of Solid State Microstructures, School of Electronic Science and Engineering, School of Physics, College of Engineering and Applied Sciences, and Collaborative Innovation Center of Advanced Microstructures, Nanjing University, Nanjing 210093, China

2. Nanjing Nanzhiguangdian Technology Co., Ltd, Nanjing 210093, China

* These authors contributed equally to this work.

+email:

xiezhenda@nju.edu.cn

gongyanxiao@nju.edu.cn

liuhuaying@nju.edu.cn

Abstract

Drone-based quantum link has the potential to realize mobile quantum network, and entanglement distribution has been demonstrated using one and two drones. Here we report the first drone-based quantum key distribution (QKD), with average secure key rate larger than 8 kHz using decoy-state BB84 protocol with polarization coding. Compact acquisition, pointing, and tracking (APT) system and QKD modules are developed and loaded on a home-made octocopter, within takeoff weight of 30 kg. A robust link is established between the flying octocopter and a ground station separated 200 meters away and real-time QKD is performed for 400 seconds. This work shows

potential of drone-based quantum communication for the future mobile quantum networks.

Keywords : Quantum communication, Quantum key distribution, Drone-based quantum network

1. Introduction

Quantum key distribution (QKD) can generate and distribute random secure keys, for the secure communication, between communication parties^[1-4]. So far, QKD has been demonstrated using fibers or satellites, to form the frame of quantum secure communication network over long distances^[5-16]. However, a practical quantum secure communication network relies on full-time all-location coverage, in a similar way to the mobile communication in classical communication technology, and the mobile quantum network is an essential supplement to fulfill such fundamental requirement^[17,18]. To build such a mobile quantum network, single photons need to be distributed to moving users, which raises requirements for the flexibility and mobility of the network node. The mobile nodes like drones are highly flexible, cost-effective and reconfigurable, which make them suitable for the mobile quantum network connection^[19,20]. Connected to the backbone network formed by fibers and satellites, drone-based quantum links have the potential to connect to users wherever needed in the world, including the moving users. Previously, drone-based quantum links have already been demonstrated for entanglement distribution, showing robust transmission of single photons^[17,18]. Basing on such high fidelity quantum link, QKD can also be expected.

Here we report the first QKD between a drone and a ground station that are separated 200 meters away. Compact and polarization-maintaining acquiring, pointing and tracking (APT) system and QKD modules are developed and loaded on a home-made octocopter, with takeoff weight of 30 kg. A robust quantum optical link is established between the octocopter and a ground station, and real-time QKD is performed for over 400 seconds with average secure key rate exceeding 8 kHz. This work proves that

quantum key distribution can be realized in drone-based quantum links, which is essential for a practical mobile quantum communication network construction.

2. Experiment scheme

In the experiment, we choose the downlink polarization-coded protocol based on decoy-state Bennett-Brassard 1984 (BB84) protocol^[21,22]. Such protocol has been used in between satellite and ground, or two stations, which may also work well in this free-space case using a drone^[6]. As shown in Fig. 1, the QKD photons are generated in a compact airborne transmitter module on the drone, working at 850 nm wavelength in 500 ps gate pulses with gate rate of 50 MHz, and the QKD signal is encoded in polarization and intensity under the BB84 protocol. Another pulse laser working at 808 nm is used to generate synchronization (SYNC) signal with the same gate.

Then the QKD photons are directed to an airborne acquiring, pointing and tracking (APT) unit, for efficient and polarization-maintaining free space transmission^[17,23]. After drone to ground transmission, the APT unit at ground station collects both the QKD photons and the SYNC signal, for detection and post-processing for the secure key generation in a receiver module. A radio-frequency (RF) channel is built between transmitter and receiver modules for classical communication, including real-time APT tracking, time synchronization and QKD post-processing.

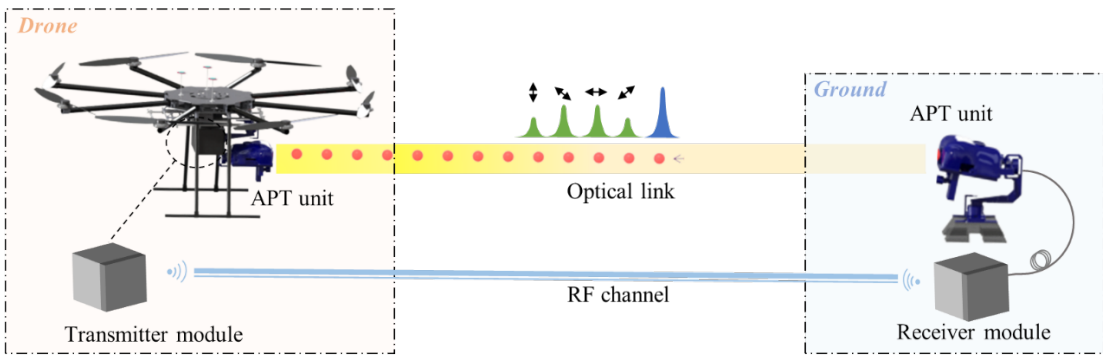


Fig. 1. Schematic of drone-based QKD. Compact QKD modules are developed and loaded on a home-made octocopter. A robust optical link is built between the drone and the ground station using acquisition, pointing, and tracking (APT) system for quantum signals (850 nm) and synchronization pulses (808 nm) transmission. Another radio-

frequency (RF) channel is also built for classical information transmission.

3. Design of QKD modules

In this experiment, we generate the decoy state BB84 signal with three intensity levels: signal $\mu_s = 0.73$, decoy $\mu_1 = 0.20$ and vacuum $\mu_2 = 0$, sent with probabilities of 50%, 25% and 25%, respectively. Two pairs of non-orthogonal polarization states $|H\rangle$, $|V\rangle$ and $|D\rangle = (|H\rangle + |V\rangle)/\sqrt{2}$, $|A\rangle = (|H\rangle - |V\rangle)/\sqrt{2}$ are used for key coding. The scheme of drone-based QKD process is shown in Fig. 2, and a pair of QKD transmitter and receiver modules are used for the QKD photon generation and detection. In the transmitter module, four fiber-coupled laser diodes (LDs) are used for signal states generation, and the other four LDs are used for decoy states generation. Both the LDs for signal and decoy states generation are identical in wavelength, and only one LD can be fired in each gate, for random generation of the signal, decoy and vacuum state with the probability ratio, under the control of an FPGA. When fired, the LDs are driven with different pulse energy for the signal and decoy state generation, following the intensity difference between them. The SYNC signal is from a fiber-coupled 808 nm LD, that is also internally modulated in the same gate pulse train.

All the LDs and the QKD control electronics are soldered in a piece of PCB board and packaged with temperature control and shock absorption before loaded on drone. For easy polarization control, the QKD photons are directed from QKD module to the APT unit using polarization-maintaining-fibers (PMFs). The four sets of signal and decoy states are combined together first and coded into two pairs of orthogonal states $|H\rangle$, $|V\rangle$ and $|D\rangle$ / $|A\rangle$ respectively through FPBS. Further encoding including combination of $|H\rangle/|V\rangle$ and $|D\rangle/|A\rangle$, and attenuation are all moved to the APT units. As only orthogonal polarization states need to be directed in each fiber, only two PMFs are used, following the optical axes of the PMF. Another SMF is used for directing SYNC signal to the APT unit, where it is combined into the weakened QKD signals to fulfil all the requirements of decoy-state BB84 protocol before distribution.

After efficient and polarization-maintaining free-space transmission via APT system, the photons are decoded in ground-based APT unit and directed to the receiver module via the same three fibers for key generation. In receiver module, two FPBS are used to separate the projected QKD photons and four identical single-photon detectors (SPDs) are used for detection. A Si-based photodetector with amplification is used for SYNC photon detection. Then all the electrical signals are dealt with a time-to-digital converter (TDC) and post-processing is accomplished between transmitter and receiver module through RF channel.

The post-processing system we used is based on the standard decoy state analysis^[21]. Secured key rate is estimated by $R \geq qp_\mu \{-Q_\mu f(E_\mu)H_2(E - \mu) + Q_1[1 - H_2(e_1)]\}$, where R is the secure key rate per pulse, $q = 1/2$ is the basis selection factor and p_μ is the probability of emitting signal states. Q_μ and E_μ are the gain and error rate of signal states, while Q_1 and e_1 are the gain and error rate of single photon states. $H_2(e)$ is the binary Shannon entropy and f is the error correction efficiency. We use low density parity check (LDPC) code for error correction. Concretely, 10% of the raw data is sampled to estimate the above parameters. After error correction and privacy amplification, the secure keys established in both parties are stored for applications.

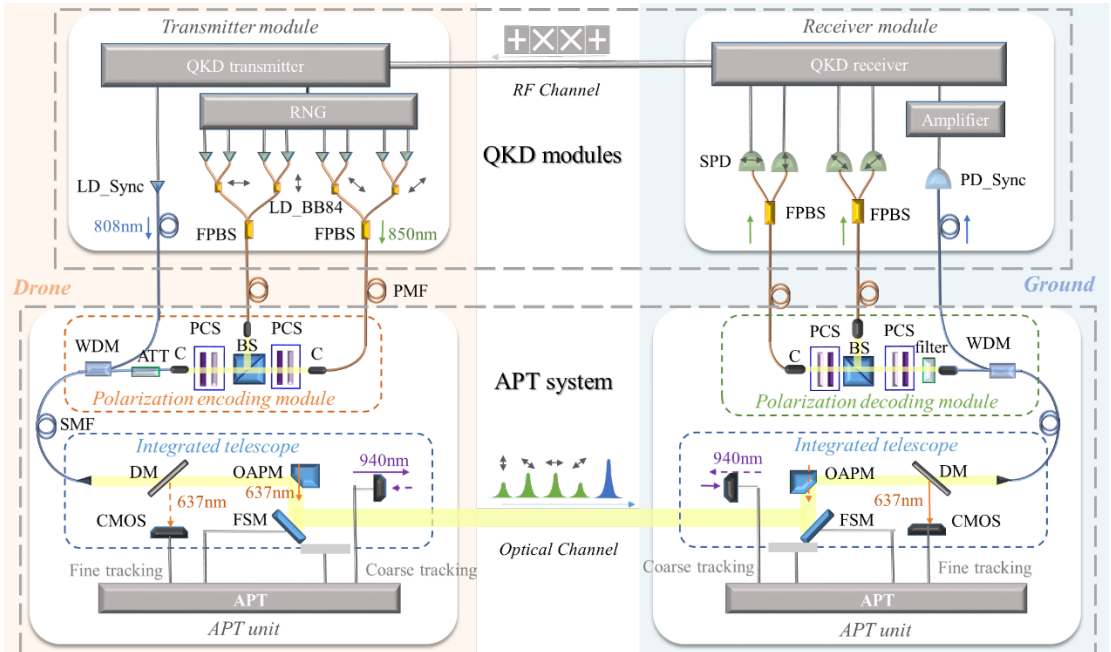


Fig. 2. Scheme of drone-based QKD process. RNG: random number generator,

LD_Sync: laser diode for time synchronization, LD_BB84: laser diode for decoy state and BB84 signal state generation, FPBS: fiber-based polarization maintain beam splitter, PMF: polarization-maintaining-fiber, C: collimator, PCS: polarization control system, BS: beam splitter, ATT: attenuator, PD_Sync: photodetector for time synchronization, WDM: wavelength division multiplexing, SMF: single-mode-fiber, DM: dichroic mirror, OAPM: off-axis parabolic mirror, CMOS: complementary metal oxide semiconductor, FSM: fast steering mirror, SPD: single-photon detector.

4. Design of APT system

To accomplish quantum key distribution between drone and ground, the key factor is to build a robust drone-to-ground quantum optical link with high efficiency and fidelity. Previously, such link has already been demonstrated via entanglement distribution between drones or drone and ground in multi-weather condition. For drone to ground QKD, distributing the gate pulsed train in multiple polarization, intensity and frequency simultaneously raises higher requirement of drone-to-ground link to keep polarization and time series stable during the whole distribution process, even in moving conditions. Thus we integrate all the elements for polarization coding, collimation and tracking into an integrated APT unit and performed two-stage tracking.

A pair of almost identical APT units is used for free-space key distribution, which is composed of a three-axis motorized gimbal stage for coarse tracking and hosting, an integrated telescope for collimation and fine tracking, and a polarization-coding unit (PCU), for QKD signal encoding/ decoding, as shown in Fig.2. As polarization encoding and tracking are performed on a same telescope plane, that is fixed to gravity direction by gimbal stage, once coded, the superposition states of QKD signals can be generated and distributed with high fidelity, and no additional compensation are needed during flight in local areas.

On drone, the QKD signals that are directed to the APT unit via PMFs first enter the polarization-encoding unit for decoy-state BB84 encoding. The two pairs of non-orthogonal states $|H\rangle/|V\rangle$ and $|D\rangle/|A\rangle$ are combined passively by a beam splitter (BS)

in free space. Two polarization compensation systems, which consists of a half wave plate and a quarter wave plate, are used to correct polarization frame with remote control. Then the superposition states of QKD signals are coupled into a SMF and weakened to single photon level through a fiber-based tunable attenuator to fulfill the protocol. The SYNC signal is combined in the same fiber through a fiber-based wavelength division multiplexing (WDM) device. Then all the signals are directed to the input fiber of the integrated telescope through a fixed SMF.

In the integrated telescope, a single off-axis parabolic mirror (OAPM) is used as primary mirror for transforming photons between SMF modes and collimated free-space modes. The beam aperture of the telescope is designed to be 26.4 mm (full width at half maximum), with corresponding Rayleigh length of about 676 m, which is sufficient for low-loss propagation in free-space distance of 200 m in the experiment. Both the QKD and SYNC photons are collimated through a same input fiber port and go through identical transmission path in free-space. Such scheme can provide more synchronous change trend for different photons under turbulence, resulting in relative stable transmission.

The integrated telescope at ground station is exactly the same as that on drone, where the QKD gate pulse train can be coupled into the output SMF in the opposite way with high efficiency. The coupled photons first transmit to a WDM, which separates the SYNC photons directly to the receiver module. The QKD photons are directed to polarization-decoding unit through SMF, where decoding with passive choice of projective bases is performed in free space. The superposition of $|H\rangle/|V\rangle$ and $|D\rangle/|A\rangle$ states are projected by the input face of two PMFs respectively, which are pre-aligned in polarization axis. Several band-pass filters are used in the decoding-module to reduce background scattering lights. After decoding, the projected photons are coupled into the two PMFs and directed to receiver module for detection and post-processing.

As for tracking, a pair of APT units is used in bi-direction. An uncollimated 940 nm laser diode (LD) is used as coarse beacon light and coarse tracking is achieved by the gimbal stage to move the telescope platform pointing to the opposite side. When the

LD signal enters the field-of-view (FOV) of the CMOS detector for coarse tracking, closed-loop feedback moves the gimbal stage in Yaw and Pitch to stabilize the target image to the CMOS center. While the Roll axis is locked by the gyroscope to gravity direction and levels polarization axis. The fine tracking is built inside the integrated telescope. A 637 nm beacon light is collimated and directed through the central hole of the OAPM. The small aperture of this beacon light results in a relatively large divergence angle and thus offers a sufficient FOV for fine tracking. While the CMOS for fine tracking is mounted at the image position of the input fiber port to a dichroic mirror (DM), which monitors the focal position of fine beacon light and generates the error signal for feeding back to a fast steering mirror (FSM). With proper feedback electronic controls, the APT units can be pointed to each other within accuracy for SMF coupling. Using this two-stage APT system, the robust optical link is established between drone and ground.

5. Drone-based QKD experiment and results

The final pictures of the drone-based QKD system is shown in Fig. 3a. We developed a home-made octocopter with eight rotors. A compact airborne transmitter module, an APT unit and an electrical control system, which is for APT electrical control are all integrated in the small drone, with takeoff weight of 30 kg and a duration time over 40 minutes. The APT unit is installed right under a center deck of the drone through rubber absorptions, with the transmitter module loaded on the left side and the electrical control cabin loaded on the right side. Two battery packs are installed on head and tail for a balanced weight distribution. A WIFI terminal used for RF channel connection is mounted on the bottom brace carbon fiber tube under the APT unit for larger FOV.

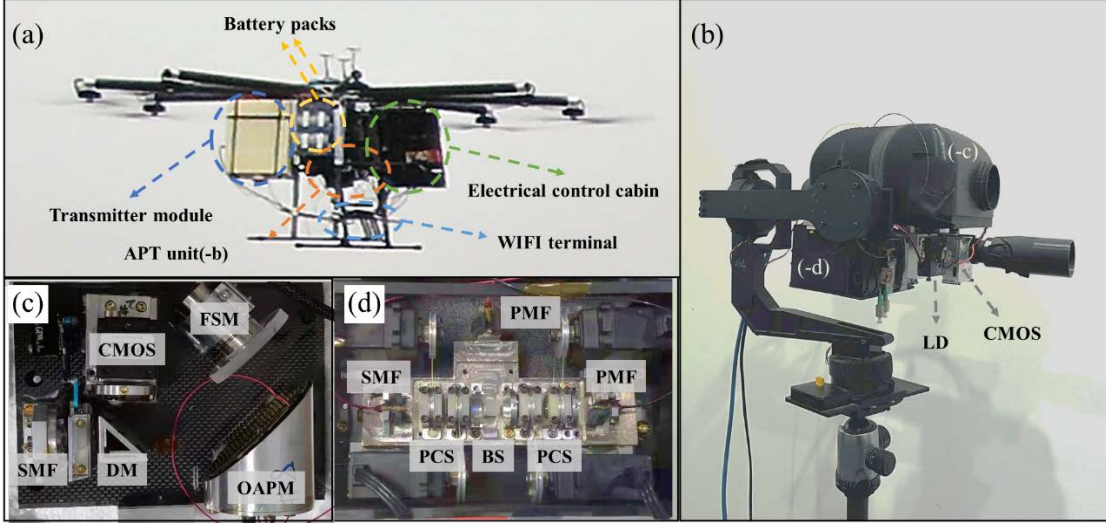


Fig. 3. Pictures of the drone-based QKD system. (a) The flying octocopter in experiment. (b) APT unit at ground station, with (c) integrated telescope and (d) polarization-encoding module in top and bottom side.

A zoom-in picture of the APT unit at ground is shown in Fig. 3b. The integrated telescope is mounted on a flat platform directly, which is made from a carbon fiber baseplate, as shown in Fig. 3c. While the polarization-coding unit is mounted on a separated detachable platform, which is then installed under the telescope upside down, as shown in Fig. 3d. Lightweight black covers are used to avoid direct exposure to dirt, rain, and background light as well as achieving better thermal stabilization.

Using the developed drone-based QKD system, we built a robust link between drone and ground station which are separated 200 meters away and performed the QKD experiment at a clear night. The optical link is built automatically through APT system and time alignment and polarization compensation is performed before flight, with polarization contrast of both non-orthogonal quantum signal sets over 30:1. After taking off, fiber-to-fiber transmission loss of drone-to-ground optical link is measured to be about 9 dB (estimated from SYNC pulses). And the overall loss for quantum signal is accumulated to be about 17.8 dB in average (estimated from quantum signal intensity change after ATT), including 3 dB from passive projection, 5 dB from detection and 0.8 dB from other optical devices.

In the experiment, the octocopter is hovering at altitude of about 10 m during flight.

We performed drone-to-ground QKD for 400 s in total. During the QKD process, the tracking errors of the APT system were recorded by onboard data logging system, with results shown in Fig. 4. The root mean square of APT tracking errors on the drone are 3.97 μm and 3.33 μm in horizon direction and vertical direction respectively. While those at ground station are 1.30 μm and 2.01 μm , respectively, which are all within the accuracy of SMF coupling, proving stable drone-to-ground photon transmission. The sampled quantum bit error rate (QBER) varies from 2.22% to 2.32% and the final averaged generation rate of sifted keys is calculated to be 8.48 kHz, which demonstrate a successful drone-to-ground quantum key distribution.

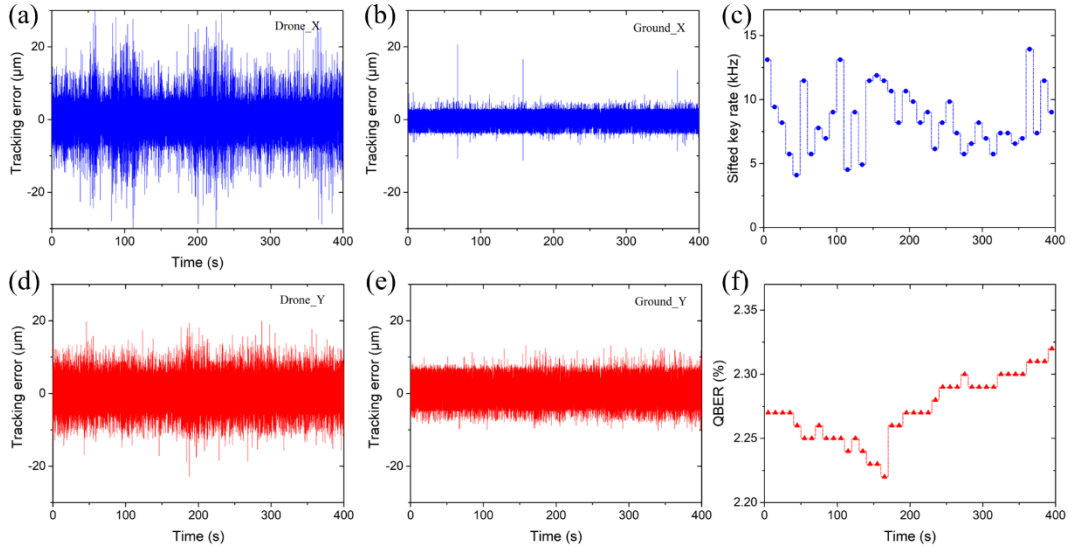


Fig. 4. Experimental results of drone-based QKD. Tracking errors in both x and y directions are recorded by onboard data logging system on drone (a)/(d) and at ground station (b)/(e) respectively. The averaged sifted key rate (c) and quantum bit error rate (QBER) (f) are calculated and displayed at every ten seconds.

7. Conclusion

In conclusion, we report the first drone-based quantum key distribution between a flying octocopter and a ground station separated 200 meters away. Compact APT system and QKD modules are developed and integrated in the small octocopter. Drone-to-ground QKD is performed for 400 seconds with average secure key rate exceed 8

kHz. The demonstration experiment reveals the feasibility of constructing mobile quantum communication network by drone platform.

Here we focus on a single key distribution between a hovering drone and ground station. In fact, the airborne QKD systems developed here also have the potential to realize QKD under moving condition if needed. Besides, by further acting as optical-relay or trusted-relay node for fast and cost-effective connection, such scheme is also capable of building mobile link between multi communication parties. In the future, using drones of various sizes, weight, speed and altitude, a practical mobile quantum network can be formed towards full-time all-location quantum communication^[17,19,24].

Data availability statement

The data that support the findings of this study are available from the corresponding author on reasonable request.

Acknowledgments

This work was supported by the National Key R&D Program of China (No. 2019YFA0705000), Key R&D Program of Guangdong Province (No. 2018B030329001), Leading-edge technology Program of Jiangsu Natural Science Foundation (No. BK20192001), National Natural Science Foundation of China (51890861, 11690033, 11974178, 62293523), Zhangjiang Laboratory (ZJSP21A001), the Excellent Research Program of Nanjing University (ZYJH002), Jiangsu Funding Program for Excellent Postdoctoral Talent, the National Postdoctoral Program for Innovative Talents (BX2021122) and China Postdoctoral Science Foundation (No. 2022M711570).

Reference:

1. F. Xu, X. Ma, Q. Zhang, H.-K. Lo, and J.-W. Pan, "Secure quantum key distribution with realistic devices," *Rev. Mod. Phys.* **92**(2), 025002 (2020).
2. E. Diamanti, H.-K. Lo, B. Qi, and Z. Yuan, "Practical challenges in quantum key distribution," *npj Quantum Inf* **2**(1), 16025 (2016).

3. H.-K. Lo, M. Curty, and K. Tamaki, "Secure quantum key distribution," *Nature Photon* **8**(8), 595–604 (2014).
4. V. Scarani, H. Bechmann-Pasquinucci, N. J. Cerf, M. Dušek, N. Lütkenhaus, and M. Peev, "The security of practical quantum key distribution," *Rev. Mod. Phys.* **81**(3), 1301–1350 (2009).
5. Q. Zhang, F. Xu, Y.-A. Chen, C.-Z. Peng, and J.-W. Pan, "Large scale quantum key distribution: challenges and solutions [Invited]," *Opt. Express* **26**(18), 24260 (2018).
6. Y.-A. Chen, Q. Zhang, T.-Y. Chen, W.-Q. Cai, S.-K. Liao, J. Zhang, K. Chen, J. Yin, J.-G. Ren, Z. Chen, S.-L. Han, Q. Yu, K. Liang, F. Zhou, X. Yuan, M.-S. Zhao, T.-Y. Wang, X. Jiang, L. Zhang, W.-Y. Liu, Y. Li, Q. Shen, Y. Cao, C.-Y. Lu, R. Shu, J.-Y. Wang, L. Li, N.-L. Liu, F. Xu, X.-B. Wang, C.-Z. Peng, and J.-W. Pan, "An integrated space-to-ground quantum communication network over 4,600 kilometres," *Nature* **589**(7841), 214–219 (2021).
7. Y. Mao, B.-X. Wang, C. Zhao, G. Wang, R. Wang, H. Wang, F. Zhou, J. Nie, Q. Chen, Y. Zhao, Q. Zhang, J. Zhang, T.-Y. Chen, and J.-W. Pan, "Integrating quantum key distribution with classical communications in backbone fiber network," *Opt. Express* **26**(5), 6010 (2018).
8. S.-K. Liao, W.-Q. Cai, J. Handsteiner, B. Liu, J. Yin, L. Zhang, D. Rauch, M. Fink, J.-G. Ren, W.-Y. Liu, Y. Li, Q. Shen, Y. Cao, F.-Z. Li, J.-F. Wang, Y.-M. Huang, L. Deng, T. Xi, L. Ma, T. Hu, L. Li, N.-L. Liu, F. Koidl, P. Wang, Y.-A. Chen, X.-B. Wang, M. Steindorfer, G. Kirchner, C.-Y. Lu, R. Shu, R. Ursin, T. Scheidl, C.-Z. Peng, J.-Y. Wang, A. Zeilinger, and J.-W. Pan, "Satellite-Relayed Intercontinental Quantum Network," *Phys. Rev. Lett.* **120**(3), 030501 (2018).
9. Y.-H. Gong, K.-X. Yang, H.-L. Yong, J.-Y. Guan, G.-L. Shentu, C. Liu, F.-Z. Li, Y. Cao, J. Yin, S.-K. Liao, J.-G. Ren, Q. Zhang, C.-Z. Peng, and J.-W. Pan, "Free-space quantum key distribution in urban daylight with the SPGD algorithm control of a deformable mirror," *Opt. Express* **26**(15), 18897 (2018).
10. A. Boaron, G. Boso, D. Rusca, C. Vulliez, C. Autebert, M. Caloz, M. Perrenoud, G. Gras, F. Bussières, M.-J. Li, D. Nolan, A. Martin, and H. Zbinden, "Secure Quantum Key Distribution over 421 km of Optical Fiber," *Phys. Rev. Lett.* **121**(19), 190502 (2018).
11. J. Yin, Y. Cao, Y.-H. Li, J.-G. Ren, S.-K. Liao, L. Zhang, W.-Q. Cai, W.-Y. Liu, B. Li, H. Dai, M. Li, Y.-M. Huang, L. Deng, L. Li, Q. Zhang, N.-L. Liu, Y.-A. Chen,

C.-Y. Lu, R. Shu, C.-Z. Peng, J.-Y. Wang, and J.-W. Pan, "Satellite-to-Ground Entanglement-Based Quantum Key Distribution," *Phys. Rev. Lett.* **119**(20), 200501 (2017).

12. H. Takenaka, A. Carrasco-Casado, M. Fujiwara, M. Kitamura, M. Sasaki, and M. Toyoshima, "Satellite-to-ground quantum-limited communication using a 50-kg-class microsatellite," *Nature Photon* **11**(8), 502–508 (2017).
13. S.-K. Liao, H.-L. Yong, C. Liu, G.-L. Shentu, D.-D. Li, J. Lin, H. Dai, S.-Q. Zhao, B. Li, J.-Y. Guan, W. Chen, Y.-H. Gong, Y. Li, Z.-H. Lin, G.-S. Pan, J. S. Pelc, M. M. Fejer, W.-Z. Zhang, W.-Y. Liu, J. Yin, J.-G. Ren, X.-B. Wang, Q. Zhang, C.-Z. Peng, and J.-W. Pan, "Long-distance free-space quantum key distribution in daylight towards inter-satellite communication," *Nature Photon* **11**(8), 509–513 (2017).
14. S.-K. Liao, W.-Q. Cai, W.-Y. Liu, L. Zhang, Y. Li, J.-G. Ren, J. Yin, Q. Shen, Y. Cao, Z.-P. Li, F.-Z. Li, X.-W. Chen, L.-H. Sun, J.-J. Jia, J.-C. Wu, X.-J. Jiang, J.-F. Wang, Y.-M. Huang, Q. Wang, Y.-L. Zhou, L. Deng, T. Xi, L. Ma, T. Hu, Q. Zhang, Y.-A. Chen, N.-L. Liu, X.-B. Wang, Z.-C. Zhu, C.-Y. Lu, R. Shu, C.-Z. Peng, J.-Y. Wang, and J.-W. Pan, "Satellite-to-ground quantum key distribution," *Nature* **549**(7670), 43–47 (2017).
15. B. Korzh, C. C. W. Lim, R. Houlmann, N. Gisin, M. J. Li, D. Nolan, B. Sanguinetti, R. Thew, and H. Zbinden, "Provably secure and practical quantum key distribution over 307 km of optical fibre," *Nature Photon* **9**(3), 163–168 (2015).
16. J.-Y. Wang, B. Yang, S.-K. Liao, L. Zhang, Q. Shen, X.-F. Hu, J.-C. Wu, S.-J. Yang, H. Jiang, Y.-L. Tang, B. Zhong, H. Liang, W.-Y. Liu, Y.-H. Hu, Y.-M. Huang, B. Qi, J.-G. Ren, G.-S. Pan, J. Yin, J.-J. Jia, Y.-A. Chen, K. Chen, C.-Z. Peng, and J.-W. Pan, "Direct and full-scale experimental verifications towards ground–satellite quantum key distribution," *Nature Photon* **7**(5), 387–393 (2013).
17. H.-Y. Liu, X.-H. Tian, C. Gu, P. Fan, X. Ni, R. Yang, J.-N. Zhang, M. Hu, J. Guo, X. Cao, X. Hu, G. Zhao, Y.-Q. Lu, Y.-X. Gong, Z. Xie, and S.-N. Zhu, "Drone-based entanglement distribution towards mobile quantum networks," *National Science Review* **7**(5), 921–928 (2020).
18. H.-Y. Liu, X.-H. Tian, C. Gu, P. Fan, X. Ni, R. Yang, J.-N. Zhang, M. Hu, J. Guo, X. Cao, X. Hu, G. Zhao, Y.-Q. Lu, Y.-X. Gong, Z. Xie, and S.-N. Zhu, "Optical-Relayed Entanglement Distribution Using Drones as Mobile Nodes," *Phys. Rev. Lett.* **126**(2), 020503 (2021).

19. S. Nauerth, F. Moll, M. Rau, C. Fuchs, J. Horwath, S. Frick, and H. Weinfurter, "Air-to-ground quantum communication," *Nature Photon* **7**(5), 382–386 (2013).
20. Y. Xue, W. Chen, S. Wang, Z. Yin, L. Shi, and Z. Han, "Airborne quantum key distribution: a review [Invited]," *Chin. Opt. Lett.* **19**(12), 122702 (2021).
21. H.-K. Lo, X. Ma, and K. Chen, "Decoy State Quantum Key Distribution," *Phys. Rev. Lett.* **94**(23), 230504 (2005).
22. Y. Zhao, B. Qi, X. Ma, H.-K. Lo, and L. Qian, "Experimental Quantum Key Distribution with Decoy States," *Phys. Rev. Lett.* **96**(7), 070502 (2006).
23. B. L. Ulich, "Overview Of Acquisition, Tracking, And Pointing System Technologies," in *Acquisition, Tracking, and Pointing II* (International Society for Optics and Photonics, 1988), **0887**.
24. S. Wehner, D. Elkouss, and R. Hanson, "Quantum internet: A vision for the road ahead," *Science* **362**(6412), eaam9288 (2018).